

Gutzwiller approximation approach to the SU(4) t - J model

Jia-Cheng He,^{*} Jie Hou, and Yan Chen[†]

Department of Physics and State Key Laboratory of Surface Physics, Fudan University, Shanghai 200433, China
(Dated: June 7, 2022)

We develop the Gutzwiller approximation method to obtain the renormalized Hamiltonian of the SU(4) t - J model with the corresponding renormalization factors. Subsequently, a mean-field theory is employed on the renormalized Hamiltonian of the model on the honeycomb lattice under the scenario of a cooperative condensation of carriers moving in the resonating valence bond state of flavors. In particular, we find that the extended s -wave superconducting state is more favorable than the $d \pm id$ -wave superconducting state in the doping range close to quarter filling. The pairing states of the SU(4) case reveal the property that the spin-singlet pairing and the spin-triplet pairing can coexist simultaneously. Our results might provide new insights into the twisted bilayer graphene system.

I. INTRODUCTION

When the resonating valence bond (RVB) state or quantum spin liquid (QSL) is doped sufficiently, the pre-existing magnetic singlet pairs of the RVB state become charged superconducting pairs. This idea is proposed for the mechanism of superconductivity of the Copper oxide superconductors [1]. Moreover, it is a usual way to realize the QSL by imposing the frustrated lattices on the SU(2) spin system. Despite many studies on this idea, it is still challenging to find the real material candidates for the QSL.

To realize the QSL, it is an alternative approach that the spin symmetry group of the electrons is extended from SU(2) to SU(N). For the sake of more substantial quantum fluctuations, we expect the QSL in SU(N) “spin” system with large N ($N > 2$) even on unfrustrated bipartite lattices, like the honeycomb lattice. The SU(2) Heisenberg model can be generalized to the SU(N) one with the consideration of orbital degeneracy in addition to spin degeneracy [2–4]. The QSL realized through orbital degeneracy can be named quantum spin-orbital liquid. With the combination of the octahedral ligand field and strong spin-orbital coupling, the SU(4) Heisenberg model on the honeycomb lattice emerges in α -ZrCl₃ at quarter filling [5]. We can naturally obtain the corresponding SU(4) t - J model by slightly doping holes on the SU(4) Heisenberg model. It is interesting whether there hosts superconducting state in the SU(4) t - J model, just like the superconductivity mechanism related to the QSL.

Recently, the discovery of the superconductivity and correlated insulating state in the twisted bilayer graphene (TBG) [6, 7] has driven a surge of theoretical works on this field [4, 8–20]. The insulating state and superconductivity are closely related to the flat bands. A sufficiently large energy gap separates these flat bands well from the excited bands. The phenomena in TBG are very like that of cuprates in many aspects. The correlated insulating

state appears at the filling of $\pm 2e$ per superlattice unit cell. After doping, the two superconducting domes are observed on both sides of the insulating state. Moreover, T_c/T_F , the ratio of the critical superconducting temperature T_c to the Fermi temperature T_F in TBG is even higher than that of cuprates, indicating very strong electron-electron interactions [6, 21]. The insulating and superconducting phases share similar energy scales [21], and this constrains models in which the superconductivity arises as a daughter-state of the insulator. Another important point of TBG is the twofold valley degeneracy, where the intervalley scattering requires a large momentum transfer compared to the mini Brillouin zone. The local density states of the flat bands in TBG are highly concentrated in the AA stacking regions, which form a triangular lattice [7]. However, according to the symmetry representations, all the triangular lattice models for TBG are ruled out [11]. Any tight-binding model proposed for TBG must correspond to Wannier orbitals forming a honeycomb lattice [8, 11]. These orbitals centered at AB/BA regions have nontrivial shapes: their weight is mainly concentrated in the AA stacking regions [8, 9, 11, 15]. A two-orbital extended Hubbard model on the honeycomb lattice may be a good starting point to study the correlated states in TBG [8, 11]. Here the honeycomb lattice model can accommodate up to eight electrons per unit cell, corresponding to the complete filling of miniband in TBG. The charge neutrality point of TBG corresponds to four electrons per unit cell in this model [8]. It is more appropriate to study the SU(4) Hubbard model or SU(4) t - J model on the honeycomb lattice, just like the Refs. [10, 17].

In addition to possible explanations for the real materials, the study of the SU(4) t - J model is a natural generalization of the famous SU(2) t - J model, which may provide a fascinating insight into unconventional superconductivity. However, similar to the SU(2) t - J model, the SU(4) t - J model is too difficult to solve analytically. The application of Gutzwiller approximation (GA) to the SU(2) t - J model is quite successful [22]. The renormalization factors of the SU(2) t - J model are essential in the solution, but the renormalization factors of the SU(4) case have been unknown due to the complexity of

^{*} jche14@fudan.edu.cn

[†] yanchen99@fudan.edu.cn

fermions possessing more than two internal components.

In this paper, our starting point is a SU(4) Hubbard model on the honeycomb lattice, with four flavors of single-electron states per site, including both the spin and the orbital. We only consider the strong correlation limit case, the SU(4) t - J model. Moreover, we develop the GA method [23] to obtain a renormalized Hamiltonian of the SU(4) t - J model with the Gutzwiller renormalization factors. Following our idea, one can easily obtain the Gutzwiller renormalization factors of the SU(N) t - J model. As shown in Fig. 1(c), the Gutzwiller renormalization factors of the SU(4) t - J model have a new property compared to the SU(2) case. Then we resort to a further mean-field approximation to analytically deal with this renormalized Hamiltonian under the scenario of the RVB state. Our numerical results found that the ground state in the doping area close to quarter filling is the extended s -wave state, and superconductivity almost disappears in the doping area close to half-filling. The pairing states of the SU(4) case reveal the property that the spin-singlet pairing and the spin-triplet pairing can exist simultaneously.

This paper is organized as follows. In Section II the model is introduced, and the renormalized Hamiltonian is derived. In Section III a mean-field theory is utilized to handle the renormalized Hamiltonian on the honeycomb lattice. Section IV presents the numerical results. The discussion and conclusion will be given in Section V.

II. THE MODEL AND THE RENORMALIZATION FACTORS

As introduced above, our starting point is a two-orbital Hubbard model on the honeycomb lattice. The SU(4) Hubbard model with four flavors of single-electron states on each site:

$$H^{SU(4)} = -t \sum_{\langle i,j \rangle} \sum_{\alpha=1}^4 (c_{i,\alpha}^\dagger c_{j,\alpha} + \text{h.c.}) + U \sum_j \left(\sum_{\alpha=1}^4 \hat{n}_{j,\alpha} \right)^2, \quad (1)$$

where $\langle i, j \rangle$ represents the nearest-neighbor sites pair and $\hat{n}_{j,\alpha} = c_{j,\alpha}^\dagger c_{j,\alpha}$. Let's consider the limit of strong correlation of the SU(4) Hubbard model, i.e., $U \gg t$, with lightly hole doping away from integer filling number $\nu_0 = 1, 2$ or 3 (i.e., the number of electrons on each site is ν_0) and follow the procedure of the perturbation theory with the trick of Fierz identity [4, 24, 25]. Then we obtain the SU(4) t - J model [4]:

$$H_{t-J}^{SU(4)} = - \sum_{\langle i,j \rangle} \sum_{\alpha=1}^4 P_G t (c_{i,\alpha}^\dagger c_{j,\alpha} + \text{h.c.}) P_G + J \sum_{\langle i,j \rangle} \sum_{a=1}^{15} \hat{T}_i^a \hat{T}_j^a, \quad (2)$$

and its wavefunction $|\Psi\rangle = P_G |\Psi_0\rangle$, where $J = t^2/4U$, $\hat{T}_i^a = \sum_{\alpha\beta} c_{i,\alpha}^\dagger \Gamma_{\alpha\beta}^a c_{i,\beta}$, Γ^a which is the generator of SU(4) group satisfying the relation $\text{Tr}(\Gamma^a \Gamma^b) = 4\delta_{ab}$, $|\Psi_0\rangle$ being unprojected wave function and P_G being the projection operator which excludes the particle occupancy states that stay at the very high energy levels arising from the Hubbard U term in Eq. (1).

Essentially the effect of P_G projection operator originates from the configuration minimizing the interaction energy (i.e., U term in Eq. (1)). We need to find the wave function configuration minimizing the interaction energy of Eq. (1) and let us call this *wave function correlation configuration*. This wave function correlation configuration is equal to $P_G |\Psi_0\rangle$. For example, in the case of hole doping away from integer filling number $\nu_0 = 2$, the wave function correlation configuration indicates that there are no triple occupancy and quadruple occupancy on each site after P_G projection, and not so obviously the wave function correlation configuration tells us the fact that empty occupancy is also excluded after P_G projection. Therefore, only single occupancy and double occupancy are allowed after P_G projection in the case of hole doping away from integer filling number $\nu_0 = 2$. Following the same steps, we can obtain the result that in the case of lightly hole doping away from integer filling number ν_0 ($\nu_0 = 1, 2$, or 3), only ν_0 occupancy and $\nu_0 - 1$ occupancy are permitted in the wave function correlation configuration.

The GA [23, 26] is a method that the correlation effect is absorbed in the renormalized factors. Here we only consider the on-site correlation effect. The GA uses the expectation value of the operator \hat{O} within the unprojected state $|\Psi_0\rangle$ multiplying a statistical weight g_O defined by $g_O \approx \langle \hat{O} \rangle_\Psi / \langle \hat{O} \rangle_{\Psi_0}$ to approximate the expectation value of the operator \hat{O} within the projected state $|\Psi\rangle = P_G |\Psi_0\rangle$. Here $\langle \dots \rangle_\Psi$ ($\langle \dots \rangle_{\Psi_0}$) represents the expectation value with respect to the wave function $|\Psi\rangle$ ($|\Psi_0\rangle$). The starting point of GA is the calculation of the probabilities for the occupancy at any site i . In this paper, for simplicity, we only consider the situation of a homogeneous wave function with fixed particle number and flavor symmetry. We need to calculate the probabilities of a site occupied by any number of electrons with different flavors. For the case of hole doping away from integer filling number ν_0 , the probabilities for different occupancies on site i in $|\Psi\rangle$ and $|\Psi_0\rangle$ are listed in Table I. We should consider five kinds of occupancies: empty occupancy, single occupancy, double occupancy, triple occupancy and quadruple occupancy as listed in the first column of Table I. We use the notation $n_{i\alpha}^0$ to represent the density before projection as listed in the third column and here we let $n_{i\alpha}^0 = n/4$ and $n = \langle \hat{n}_i \rangle_\Psi = 4 \langle \hat{n}_{i\alpha} \rangle_\Psi$ with $\hat{n}_i = \sum_{\alpha} \hat{n}_{i\alpha}$.

Using Table I and following the procedure of GA, we can obtain the renormalization factors related to the statistical weight ratios and remember that the ratio g_O should be calculated by considering the probability amplitudes of “bra” and “ket” configurations that con-

TABLE I. Probabilities of different occupancies for the case of hole doping away from integer filling number ν_0 ($\nu_0 = 1, 2$ or 3) for the SU(4) t - J model. $n_{i,\alpha}^0$ represents the density before projection and here we let $n_{i,\alpha}^0 = n/4$ and $n = \langle \hat{n}_i \rangle_\Psi = 4\langle \hat{n}_{i,\alpha} \rangle_\Psi$ with $\hat{n}_i = \sum_\alpha \hat{n}_{i,\alpha}$.

Occupancy on site i	Probabilities in $ \Psi\rangle$	Probabilities in $ \Psi_0\rangle$
$\langle \prod_{x=1}^{\nu_0} \hat{n}_{ix} \prod_{y=\nu_0+1}^4 (1 - \hat{n}_{iy}) \rangle$	$\frac{1-\nu_0+n}{C_4^{\nu_0}}$	$\prod_{x=1}^{\nu_0} n_{ix}^0 \prod_{y=\nu_0+1}^4 (1 - n_{iy}^0)$
$\langle \prod_{x=1}^{\nu_0-1} \hat{n}_{ix} \prod_{y=\nu_0}^4 (1 - \hat{n}_{iy}) \rangle$	$\frac{\nu_0-n}{C_4^{\nu_0-1}}$	$\prod_{x=1}^{\nu_0-1} n_{ix}^0 \prod_{y=\nu_0}^4 (1 - n_{iy}^0)$
$\langle \prod_{x=1}^{\rho \neq \nu_0, \nu_0-1} \hat{n}_{ix} \prod_{y=\rho+1}^4 (1 - \hat{n}_{iy}) \rangle$	0	$\prod_{x=1}^{\rho \neq \nu_0, \nu_0-1} n_{ix}^0 \prod_{y=\rho+1}^4 (1 - n_{iy}^0)$

tribute [26]. For the case of hole doping away from integer filling number ν_0 , following the procedure of GA we can obtain the relation about the hopping term $\langle c_{i,\alpha}^\dagger c_{j,\alpha} \rangle_\Psi \approx g_t^{SU(4)}(n, \nu_0) \langle c_{i,\alpha}^\dagger c_{j,\alpha} \rangle_{\Psi_0}$, where

$$g_t^{SU(4)}(n, \nu_0) = \frac{\nu_0(5 - \nu_0)[n - (\nu_0 - 1)](\nu_0 - n)}{n(4 - n)}, \quad (3)$$

is the renormalization factor for hopping terms. The corresponding hopping progress is described by Fig. 1(a) as $\nu_0 = 2$ case. In Fig. 1(a) α_0 , α_1 and β_1 represent the flavors of electrons, where α_0 is different from both α_1 and β_1 . Then, we consider the interaction term $\sum_{a=1}^{15} \hat{T}_i^a \hat{T}_j^a$ which can be rewritten as $\sum_{a=1}^{15} \hat{T}_i^a \hat{T}_j^a = \frac{1}{2} \sum_{m < n} (\hat{T}_i^{mn+} \hat{T}_j^{mn-} + \hat{T}_i^{mn-} \hat{T}_j^{mn+}) + \sum_{l=1}^3 \hat{T}_i^l \hat{T}_j^l$ where $\hat{T}_i^{mn+} = \sqrt{8} c_{im}^\dagger c_{in}$, $\hat{T}_i^{mn-} = \sqrt{8} c_{in}^\dagger c_{im}$ and $\hat{T}_i^l = \sqrt{8} \sum_{\alpha\beta} c_{i\alpha}^\dagger T_{\alpha\beta}^{l+1} c_{i\beta}$, $T^2 = \text{diag}\{1, -1, 0, 0\}/\sqrt{4}$, $T^3 = \text{diag}\{1, 1, -2, 0\}/\sqrt{12}$, $T^4 = \text{diag}\{1, 1, 1, -3\}/\sqrt{24}$. We should keep in mind that when we calculate the renormalized factors about the interaction term we suppose lightly hole doping away from integer filling number ν_0 , because this is the precondition from Hubbard model to obtain the J term. Therefore we obtain $\langle \hat{T}_i^{mn+} \hat{T}_j^{mn-} \rangle_\Psi \approx g_S^{SU(4)}(n, \nu_0) \langle \hat{T}_i^{mn+} \hat{T}_j^{mn-} \rangle_{\Psi_0}$, where

$$g_S^{SU(4)}(n, \nu_0) = \left[\frac{1 - \nu_0 + n}{C_4^{\nu_0} \left(\frac{n}{4}\right)^{\nu_0} \left(1 - \frac{n}{4}\right)^{4-\nu_0}} \right]^2. \quad (4)$$

For $\langle \hat{T}_i^{mn+} \hat{T}_j^{mn-} \rangle_\Psi$ term the corresponding flavor exchange progress is described by Fig. 1(b) as $\nu_0 = 2$ case. In Fig. 1(b) m , n , α_1 and β_1 represent the flavors of electrons, where α_1 (β_1) is different from both m and n . And one can prove that $\langle \hat{T}_i^l \hat{T}_j^l \rangle_\Psi = g_S^{SU(4)}(n, \nu_0) \langle \hat{T}_i^l \hat{T}_j^l \rangle_{\Psi_0}$. Namely, $g_S^{SU(4)}(n, \nu_0)$ is the renormalization factor for the interaction terms. $g_t^{SU(4)}(n, \nu_0)$ as the function of electron density n is shown in Fig. 1(c). Since the SU(4) Hubbard model described by Eq. (1) has particle-hole symmetry, both $g_t^{SU(4)}(n, \nu_0)$ and $g_S^{SU(4)}(n, \nu_0)$ are symmetric about the point $n = 2$. In Fig. 1(c), $g_t^{SU(4)}$ is zero

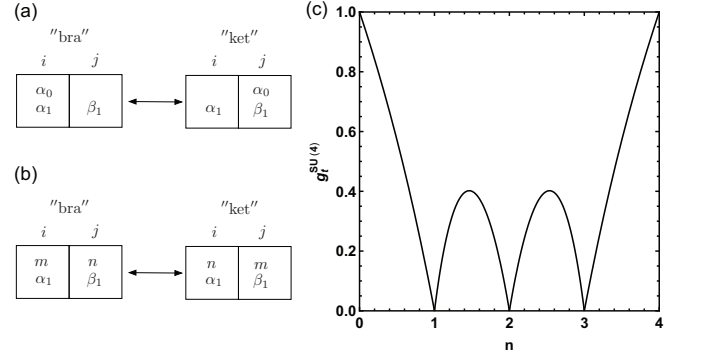


FIG. 1. (a) The permitted hopping progress in the case of hole doping away from integer filling number $\nu_0 = 2$, where α_0 is different from both α_1 and β_1 . (b) The permitted flavor exchange progress in the case of hole doping away from integer filling number $\nu_0 = 2$, where α_1 (β_1) is different from both m and n . (c) $g_t^{SU(4)}(n, \nu_0)$ as the function of electron density n is symmetric about the point $n = 2$.

at integer filling numbers $\nu_0 = 1, 2, 3$ corresponding to the Mott insulating states. It enables the renormalization factor $g_t^{SU(4)}$ nonmonotonic that the emergent flavors fluctuation background arises in the cases of $\nu_0 = 2$ and $\nu_0 = 3$. The underlying physics of the nonmonotonic property is that the flavors background plays both the role increasing the resource of mobile electrons and the role blocking the movement of mobile electrons. Thus we obtain the renormalized Hamiltonian

$$H' = -t g_t^{SU(4)} H_t + J g_S^{SU(4)} H_S, \quad (5)$$

where $H_t = \sum_{\langle i,j \rangle} \sum_{\alpha=1}^4 (c_{i,\alpha}^\dagger c_{j,\alpha} + \text{h.c.})$ and $H_S = \sum_{\langle i,j \rangle} \sum_{a=1}^{15} \hat{T}_i^a \hat{T}_j^a$.

III. THE BOGOLIUBOV-DE GENNES METHOD

We propose that the RVB state is the ground state of the SU(4) t - J model on the honeycomb lattice near the integer filling number. Before proceeding further, let

us examine the interaction term of the SU(4) t - J model. With the help of Fierz identity the interaction term can be rewritten as [4]

$$\sum_{a=1}^{15} \hat{T}_i^a \hat{T}_j^a = -\frac{5}{4} \left(\vec{\Delta}_{ij} \right)^\dagger \cdot \vec{\Delta}_{ij} + \frac{3}{4} \left(\Delta_{ij}^- \right)^\dagger \cdot \Delta_{ij}^-, \quad (6)$$

where $\vec{\Delta}_{ij}$ and Δ_{ij}^- are the pairing fields with 6 and 10 components, respectively. $\vec{\Delta}_{ij}$ is the even pairing field satisfying the relation $\vec{\Delta}_{ij} = \vec{\Delta}_{ji}$ and Δ_{ij}^- is the odd pairing field satisfying the relation $\Delta_{ij}^- = -\Delta_{ji}^-$. $\vec{\Delta}_{ij}$ and Δ_{ij}^- have $SO(6)$ rotation symmetry and $SO(10)$ rotation symmetry, respectively. Using v_1 and v_2 as the orbital index and choosing a representation we can obtain $\vec{\Delta}_{ij} = \tilde{c}_i^t (-\sigma^{32}, i\sigma^{02}, \sigma^{12}, -\sigma^{23}, i\sigma^{20}, \sigma^{21}) \tilde{c}_j$ and $\Delta_{ij}^- = \tilde{c}_i^t \left(-\sigma^{22}, \vec{\sigma}_\tau \otimes \vec{\sigma}_\tau \right) \tilde{c}_j$, where $\tilde{c}_j = (c_{j\uparrow v_1}, c_{j\uparrow v_2}, c_{j\downarrow v_1}, c_{j\downarrow v_2})^t$, $\sigma^{ab} = \sigma^a \otimes \sigma^b$, $\sigma^0 = \mathbf{1}_{2 \times 2}$ and $\vec{\sigma}_\tau \otimes \vec{\sigma}_\tau$ being dyadic tensor with $\vec{\sigma}_\tau = i\hat{\sigma}^2$ and $\hat{\sigma} = \sigma^1 \hat{e}_1 + \sigma^2 \hat{e}_2 + \sigma^3 \hat{e}_3$. About $\vec{\Delta}_{ij}$ the previous three components describe spin-triplet with orbital-singlet pairing field and the last three components describe spin-singlet with orbital-triplet pairing field. For Δ_{ij}^- the first component describes spin-singlet with orbital-singlet pairing field and the last nine components describe spin-triplet with orbital-triplet pairing field.

With the consideration of pairing order parameters $\Delta_{\langle i,j \rangle, \alpha\beta} = \langle \Psi_0 | c_{i,\alpha} c_{j,\beta} | \Psi_0 \rangle$ we take the expectation value of Eq. (6) and obtain $-\frac{5}{4} \left(\langle \vec{\Delta}_{ij} \rangle_0 \right)^\dagger \cdot \langle \vec{\Delta}_{ij} \rangle_0$, where $\langle \vec{\Delta}_{ij} \rangle_0 = \langle \Psi_0 | \vec{\Delta}_{ij} | \Psi_0 \rangle$. Here we neglect the contribution from Δ_{ij}^- due to $J > 0$. $\langle \vec{\Delta}_{ij} \rangle_0$ describes the *smearing* of the pseudo-Fermi surface but is not the superconducting order parameter [23]. Following the procedure of GA, for the nearest-neighbor sites i and j , the quantity related to the superconducting order parameter is given by

$$\langle c_{i,\alpha} c_{j,\beta} \rangle_\Psi = g_t^{SU(4)}(n, \nu_0) \langle c_{i,\alpha} c_{j,\beta} \rangle_{\Psi_0}. \quad (7)$$

With the help of Fierz identity the interaction term can also be rewritten as

$$\begin{aligned} \sum_{a=1}^{15} \hat{T}_i^a \hat{T}_j^a &= -\frac{15}{4} \sum_{\alpha} c_{j\alpha}^\dagger c_{i\alpha} \sum_{\beta} c_{i\beta}^\dagger c_{j\beta} \\ &+ \frac{1}{4} \sum_{a=1}^{15} \sum_{\alpha\beta} c_{j\alpha}^\dagger \Gamma_{\alpha\beta}^a c_{i\beta} \sum_{\delta\gamma} c_{i\delta}^\dagger \Gamma_{\delta\gamma}^a c_{j\gamma}. \end{aligned} \quad (8)$$

Here we also consider the kinetic energy order parameters $\chi_{\langle i,j \rangle, \alpha} = \langle \Psi_0 | c_{i\alpha}^\dagger c_{j\alpha} | \Psi_0 \rangle$ [23, 27] and take the expectation value of Eq. (8) to obtain $-\frac{15}{4} \sum_{\alpha} \chi_{\langle i,j \rangle, \alpha}^* \sum_{\beta} \chi_{\langle i,j \rangle, \beta}$. The expectation value of the second term in Eq. (8) is zero due to the flavor symmetry in our theory. Since the RVB state allows the singlet pairs to move [1] (the flavor singlet pairs resemble the spin-singlet pairs), the kinetic energy

order parameters describe the kinetic energy of the RVB state. For simplicity, in this paper, we only consider real $\chi_{\langle i,j \rangle, \alpha}$.

On the honeycomb lattice, we denote by d and c the electron annihilation operators related to the A and B sublattices of the honeycomb lattice, respectively. We redefine the pairing order parameter:

$$\tilde{\Delta}_{\alpha\beta}^{\vec{\tau}} = \langle \Psi_0 | c_{\mathbf{R}_i + \vec{\tau}, \alpha} d_{\mathbf{R}_i, \beta} - c_{\mathbf{R}_i + \vec{\tau}, \beta} d_{\mathbf{R}_i, \alpha} | \Psi_0 \rangle. \quad (9)$$

Here $\vec{\tau}_m$ (with $m = 1, 2, 3$) denotes the three nearest neighbour bond directions of the A site. Therefore, the superconducting order parameter is given by

$$\begin{aligned} \tilde{\Delta}_{SC, \alpha\beta}^{\vec{\tau}} &= \langle c_{\mathbf{R}_i + \vec{\tau}, \alpha} d_{\mathbf{R}_i, \beta} - c_{\mathbf{R}_i + \vec{\tau}, \beta} d_{\mathbf{R}_i, \alpha} \rangle_\Psi \\ &= g_t^{SU(4)}(n, \nu_0) \tilde{\Delta}_{\alpha\beta}^{\vec{\tau}}. \end{aligned} \quad (10)$$

We use the parameter φ to represent the phase difference between the pairing order parameters on the three nearest neighbour bonds, namely, $\tilde{\Delta}_{\alpha\beta}^{\vec{\tau}_2} = e^{i\varphi} \tilde{\Delta}_{\alpha\beta}^{\vec{\tau}_1}$ and $\tilde{\Delta}_{\alpha\beta}^{\vec{\tau}_3} = e^{i2\varphi} \tilde{\Delta}_{\alpha\beta}^{\vec{\tau}_1}$. $\varphi = 2\pi/3$ yields the $d \pm id$ state and $\varphi = 0$ yields the extended s -wave state.

According to crystal field theory, in the two-dimensional hexagonal lattice there are two reasonable and favorable irreducible representations for even-parity gap functions (recall that we only consider even pairing fields and here we set $k_z = 0$). The first is the one-dimensional representation and its basis functions can be chosen as 1 or $k_x^2 + k_y^2$ which can yield the extended s -wave. The second is the two-dimensional representation and its basis functions consist of $k_x^2 - k_y^2$ and $2k_x k_y$. The best equal weight combination of degenerate states $k_x^2 - k_y^2$ and $2k_x k_y$ yields the $d \pm id$ state [28, 29]. Our treatment is limited to zero temperature and thus we can obtain the self consistent equations for the order parameters

$$\begin{aligned} \tilde{\Delta}_{\alpha\beta} &= \tilde{\Delta}_{\alpha\beta}^{\vec{\tau}_1}, \\ \chi &= \sum_{\alpha} (\chi_{\langle i,j \rangle, \alpha} + \chi_{\langle i,j \rangle, \alpha}^*) / 2, \\ n &= \sum_{\alpha} \langle \Psi_0 | d_{\mathbf{R}_i, \alpha}^\dagger d_{\mathbf{R}_i, \alpha} + c_{\mathbf{R}_i + \vec{\tau}_1, \alpha}^\dagger c_{\mathbf{R}_i + \vec{\tau}_1, \alpha} | \Psi_0 \rangle / 2, \end{aligned} \quad (11)$$

by their expressions with respect to Bogoliubov transformation matrices $\hat{u}^{\mathbf{k}}$ and $\hat{v}^{\mathbf{k}}$. More details can be found in Appendix A.

IV. NUMERICAL RESULTS

Here we only concentrate on numerical results about the cases of hole doping away from integer filling number $\nu_0 = 1$ (corresponding to quarter filling) and $\nu_0 = 2$ (corresponding to half-filling). $t = 1$ and $J/t = 0.3/8$ are chosen for calculations. We obtained the extended s -wave state and the $d \pm id$ state, and here “extended s -wave” and “ $d \pm id$ ” describe the orbital part of the

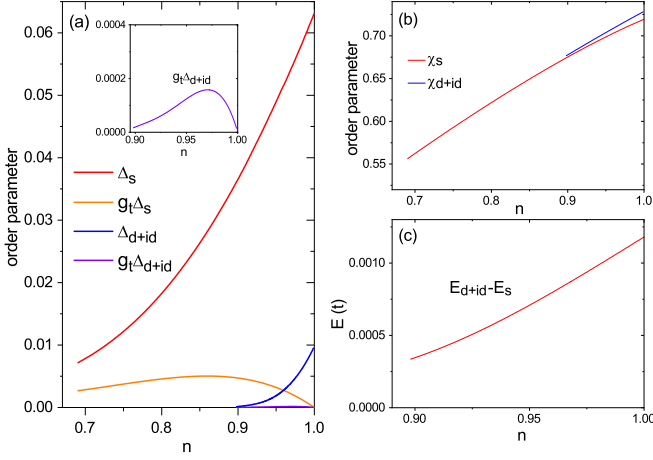


FIG. 2. The case for the extended s -wave state and the $d \pm id$ state scenarios below quarter filling. Here we choose $t = 1$ and $J/t = 0.3/8$. (a) The electron density dependence of flavor gaps, Δ_s and Δ_{d+id} (defined in Eq. (11)), at zero temperature and superconducting order parameters, $g_t\Delta_s$ and $g_t\Delta_{d+id}$ (g_t is defined in Eq. (3)), both their behaviors have the dome structure. (Inset) The enlargement of that of the $d \pm id$ state for clarity. (b) The electron density dependence of kinetic energy order parameters, χ_s and χ_{d+id} . (c) The difference in the total energy (per site) between the $d \pm id$ state and the extended s -wave state, namely, $\Delta E = E_{d+id} - E_s$, where E_{d+id} and E_s are the total energies (given by Eq. (A1)) per site (in units of t) of the $d \pm id$ state and the extended s -wave state, respectively.

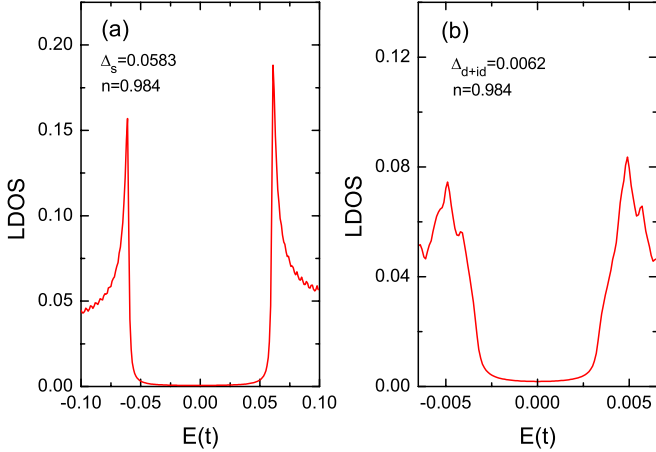


FIG. 3. LDOS versus E (in units of t). (a) The case of the extended s -wave state with the broadening factor $\eta = 0.001t$ and electron density $n = 0.984$. (b) The case of the $d \pm id$ state with the broadening factor $\eta = 0.0002t$ and electron density $n = 0.984$.

pairing. In addition to $U(1)$ symmetry, the time reversal symmetry of the $d \pm id$ state is also broken and this is a prominent difference with respect to the extended s -wave. In our numerical calculations we only found the flavor antisymmetric states $\tilde{\Delta}_{\alpha\beta} = -\tilde{\Delta}_{\beta\alpha}$ ($\alpha \neq \beta$) and this can be easily understood from its

definition. The states in this paper all belong to the flavor configuration: $\tilde{\Delta} = \tilde{\Delta}_{12} = \tilde{\Delta}_{34} = \tilde{\Delta}_{14} = \tilde{\Delta}_{23} = \tilde{\Delta}_{13} = -\tilde{\Delta}_{24}$. This flavor configuration corresponds to $\langle \tilde{\Delta}_{\mathbf{R}_i+\tilde{\tau}_1, \mathbf{R}_i} \rangle_0 = (0, 2\tilde{\Delta}, 0, 2i\tilde{\Delta}, 0, -2i\tilde{\Delta}) = \langle \tilde{c}_i^\dagger (0, i\sigma^{02}, 0, -\sigma^{23}, 0, \sigma^{21}) \tilde{c}_j \rangle_0$ which indicates the spin singlet pairing and the spin triplet pairing exist simultaneously in this flavor configuration. More detail about the physical meaning of the flavor configuration can be found in Appendix B. As a matter of fact, let's make a multiplication of phase factors to four kinds of electrons with different flavors, i.e., $c_1 \rightarrow c'_1 = c_1 e^{i(\theta_1+\theta_2+2\theta_4)/2}$, $c_2 \rightarrow c'_2 = c_2 e^{i(\theta_1-\theta_3+2\theta_4)/2}$, $c_3 \rightarrow c'_3 = c_3 e^{i(\theta_2-\theta_3+2\theta_4)/2}$, and $c_4 \rightarrow c'_4 = c_4 e^{i\theta_4}$. Then we obtain $\tilde{\Delta}_{12} = e^{-i\theta_1} \tilde{\Delta}_{34}$, $\tilde{\Delta}_{14} = e^{-i\theta_3} \tilde{\Delta}_{23}$, and $\tilde{\Delta}_{13} = -e^{-i\theta_2} \tilde{\Delta}_{24}$. This indicates there are a large number of degenerate states arising from the flavor phase degrees of freedom between different flavor pairing fields. These degenerate states can be transformed into each other by the gauge transformation listed above, and therefore we only need to study one flavor configuration.

For the case of hole doping away from quarter filling, the electron density dependence of the pairing order parameter (RVB gap or flavor gap) is shown in Fig. 2(a), and here we denote $\Delta_s = \tilde{\Delta}_{12}$ and $\Delta_{d+id} = \tilde{\Delta}_{12}$ for the extended s -wave state and the $d \pm id$ state, respectively. The quantity $g_t\Delta$ describes the superconducting order parameter. As shown in Fig. 2(a), in a whole doping region close to quarter filling, the magnitude of the pairing order parameter and the superconducting order parameter of the extended s -wave state is substantially higher than that of the $d \pm id$ state. As a function of doping $\delta = 1 - n$, both of the behaviors for $g_t\Delta$ of the extended s -wave state and of the $d \pm id$ state have a dome structure. $g_t\Delta$ vanishes linearly near $\delta = 0$. The quantity $g_t\Delta$ can be understood as an approximate superconducting transition temperature T_c [30, 31]. Their corresponding behaviors of the electron density dependence of the kinetic energy order parameter are shown in Fig. 2(b), and here we denote $\chi_s = \chi$ and $\chi_{d+id} = \chi$ for the extended s -wave state and the $d \pm id$ state, respectively. The total energy of the extended s -wave state is evidently lower than that of the $d \pm id$ state in the whole doping region, as shown in Fig. 2(c). Here E_{d+id} and E_s are the total energies (given by Eq. (A1)) per site of the $d \pm id$ state and the extended s -wave state, respectively. Therefore, the extended s -wave state is the dominant pairing state in the case of hole doping away from quarter filling.

We also calculated the local density of states (LDOS) of the extended s -wave state and the $d \pm id$ state in the doping region close to the integer filling number $\nu_0 = 1$ as shown in Fig. 3. From the LDOS diagram it is obvious that both the extended s -wave state and the $d \pm id$ state are fully gapped. Here the LDOS is calculated by $g_t^{SU(4)} \sum_{\alpha} A_{\alpha}^i(\omega)$, where $\langle c_{i,\alpha}^{\dagger} c_{i,\alpha} \rangle_{\Psi_0} = \int_{-\infty}^{\infty} \frac{A_{\alpha}^i(\omega)}{e^{\hbar\omega/k_B T} + 1} d\omega$.

For the case of hole doping away from half-filling, as

shown in Fig. 4(a), the values of the pairing order parameter and the superconducting order parameter of the extended s -wave state are exactly equal to zero in the whole doping region presented in the figure, which corresponds to the uniform RVB (u-RVB) state [32]. Therefore, the extended s -wave state does not exist in this doping region. Since the values of Δ_{d+id} and of $g_t\Delta_{d+id}$ are exactly equal to zero in the region of $1.9552 \leq n \leq 2$, the $d \pm id$ state does not arise until doping more than $\delta = 1 - n \approx 0.045$. However, note that the values of the left axis of Fig. 4(a) need to be multiplied by a factor 10^{-3} and the maximum magnitude of Δ_{d+id} is around 10^{-3} in the presented doping region. Thus the values of Δ_{d+id} are negligible in this doping region. Note that the magnitudes of Δ_{d+id} in this doping region are also much smaller than that of Δ_{d+id} in the case of doping region close to quarter filling. Therefore, the superconductivity in this doping region can be neglected. The corresponding kinetic energy order parameters, χ_s and χ_{d+id} , behave identically as shown in Fig. 4(b). The total energy of the $d \pm id$ state is slightly lower than that of the u-RVB state, as shown in Fig. 4(c). Therefore, near half-filling, the $d \pm id$ state is more favorable in the doping region where Δ_{d+id} is non-vanishing. Moreover, It can be inferred, from the negligible values of Δ_{d+id} and $\Delta_s = 0$ near half-filling, that the pairing fields are unstable in this doping region.

V. DISCUSSION AND CONCLUSION

Since there is a considerable overlap between the nodes of the $d \pm id$ form factor and the Fermi surface near quarter filling [30], one could anticipate the free energy of the $d \pm id$ state will be higher than that of the extended s -wave state. This may explain that in a whole doping region close to quarter filling, the extended s -wave state is much more favorable than the $d \pm id$ state. Moreover, there is almost no superconductivity in the doping range close to half-filling, in contrast with the SU(2) case where the $d \pm id$ state is more favorable than the extended s -wave state close to half-filling [30]. The flavor fluctuation effect in the SU(4) t - J model being more substantial than the SU(2) case and the low electron density close to half-filling should be the reasons. On the other hand, the pairing field $\vec{\Delta}_{ij}$ is formed by four fermions rather than two fermions, which also makes the pairing fields unstable in the low filling region.

Next we discuss the relevance of our results to TBG. For TBG, the microscopic two-orbital extended Hubbard model on the emergent honeycomb lattice [8], constructed from band structure calculations projected to low-energy bands and the analysis of energy bands at all high symmetry points, is more complicated than the simplest two-orbital honeycomb Hubbard model studied here. Our model does not include some terms of band structure details and pair-hopping interaction terms. The simplified model used here might provide a

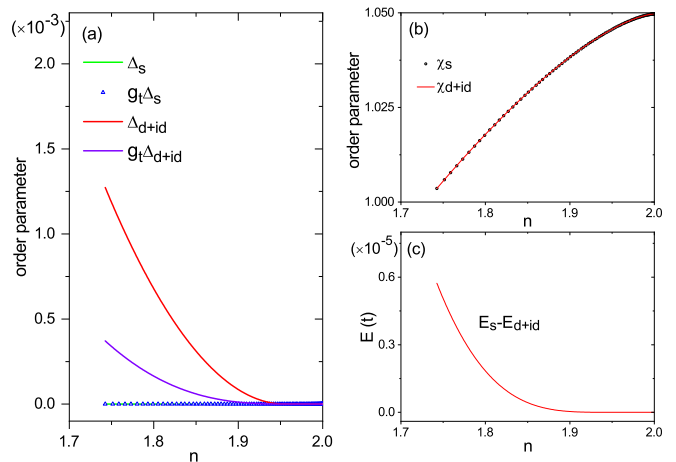


FIG. 4. The case for the extended s -wave state and the $d \pm id$ state scenarios below half-filling. (a) The electron density dependence of flavor gaps, Δ_s and Δ_{d+id} (defined in Eq. (11)), at zero temperature and superconducting order parameters, $g_t\Delta_s$ and $g_t\Delta_{d+id}$ (g_t is defined in Eq. (3)). Note that the values of left axis need to be multiplied by 10^{-3} . Here the values of Δ_s and of $g_t\Delta_s$ are exactly equal to zero in the given doping region, which corresponds to the u-RVB state [32]. The values of Δ_{d+id} and of $g_t\Delta_{d+id}$ are exactly equal to zero in the region of $1.9552 \leq n \leq 2$. (b) The kinetic energy order parameters behave identically for the extended s -wave state and the $d \pm id$ state. (c) The difference in the total energy (per site) between the extended s -wave state and the $d \pm id$ state, namely, $\Delta E = E_s - E_{d+id}$, where E_{d+id} and E_s are the total energies (given by Eq. (A1)) per site (in units of t) of the $d \pm id$ state and the extended s -wave state, respectively. Note that the values of left axis need to be multiplied by 10^{-5} , and the values of ΔE are exactly equal to zero in the region of $1.9552 \leq n \leq 2$ and positive below the doping region $n < 1.9552$. Since the values of ΔE are negligible small, the total energy of the $d \pm id$ state is almost the same with that of the u-RVB state.

reference point for understanding the correlated electron physics in TBG. Due to TBG's similarity to the cuprates, the large U regime of the SU(4) honeycomb Hubbard model is important for TBG.

Based on the real-space density matrix renormalization group (DMRG) simulation, the metal-insulator transition around $U_c/t = 2.5-3$ and a nonmagnetic Mott insulator in the large U regime are identified in the two-orbital Hubbard model on the honeycomb lattice (i.e., Eq. (1)) at quarter filling. Moreover, the featureless nonmagnetic Mott insulator has no signs of charge and spin-orbital density wave fluctuations or orders [10]. Corresponding to $J/t = 0.3/8$ used in our work, $U/t = 20/3$ is consistent with the large U regime. At quarter filling, the RVB state as the trial wavefunction in our work is also featureless nonmagnetic state.

The RVB state is of rare occurrence in Mott insulators. However, the RVB superconducting state may be realized by introducing a finite number of holes into the Mott insulator [26]. The pairing of the RVB state directly

originates from the superexchange of the Mott insulator. As shown in Fig. 2(a), the feature of the superconducting dome in our results in the vicinity of quarter filling is consistent with that of the superconductivity observed in TBG [6]. Corresponding to the region around the charge neutrality point of TBG, the superconducting state does not exist in the case of hole doping away from half-filling, which is also consistent with TBG experiments. Therefore, the scenario of the RVB state might provide an appropriate description for the states observed in TBG.

For comparing with other studies of the pairing in TBG, we remark that the spin-singlet and spin-triplet Cooper pairs are not sharply defined for our extended s -wave and $d \pm id$ pairing due to the SU(4) symmetry. In TBG, it is important to consider the effects of SU(4) symmetry-breaking perturbations on the honeycomb Hubbard model. We assume that the dominant interaction is the Hund's coupling $-V \sum_i (\mathbf{S}_i)^2$, where $V > 0$ and \mathbf{S}_i denotes the total spin on site i . Then the previous three components of $\vec{\Delta}_{ij}$ defined in Eq. (6) (i.e., the spin-triplet and orbital-singlet pairing field) is more favorable [4]. Consequently, the extended s -wave pairing and the $d \pm id$ pairing obtained in our study are more favorable in spin-triplet and orbital-singlet. The parity of the pair can also exchange the two orbitals (valleys) of TBG, and thus, in the large microscopic Brillouin zone, the even-parity extended s -wave state and the even-parity $d \pm id$ state become the odd-parity p -wave state and the odd-parity $f \pm if$ state, respectively, according to orbital-singlet. Therefore, we infer that the spin-triplet p -wave superconductivity is dominant in the vicinity of quarter-filling (two electrons per superlattice unit cell) in TBG, according to Fig. 2. This is different from the results of Ref. [4], where the spin-triplet $f \pm if$ pairing in the large Brillouin zone, is proposed for TBG by the SU(4) t - J model on the triangular lattice near half-filling, with the Hund's coupling. Our spin-triplet p -wave pairing is similar to that in Ref. [16], where the superconductivity in TBG is explained as a consequence of the Kohn-Luttinger instability. In Ref. [17], based on the functional renormalization group (FRG) techniques, the $d \pm id$ pairing near quarter-filling is found on the simplest two-orbital honeycomb Hubbard model (i.e, Eq. (1)) at the moderate $U/t = 2$. Their $d \pm id$ pairing occurs between (\uparrow , p_x orbital, lower band) and (\downarrow , p_y orbital, lower band), and this restriction of the pairing between particles with opposing quantum numbers does not exist in our study. This state corresponds to a single component of the $d \pm id$ pairing in the mini Brillouin zone with flavor structure near quarter-filling in our study. In Ref. [18], a spin-triplet and orbital-singlet f -wave pairing is found on the two-orbital extended Hubbard model on the honeycomb lattice near quarter-filling from weak to moderate coupling, which introduces a warping hopping term with the f -wave factor and the Hund's coupling term to break the SU(4) symmetry.

The Gutzwiller approximation adopted in our present study is a conventional method to treat the strong cor-

relation problem. The homogeneous electron density and the flavor symmetry are assumed. For studying the charge density wave stability, the spin-orbital density wave stability, and the local effects due to vortex cores and impurities, the more complicated renormalization factors derived from the case of the inhomogeneous particle density, are much demanded. Furthermore, the more complicated two-orbital extended Hubbard model for TBG can be studied by this technique. We leave these studies to future work.

In summary, we obtain the Gutzwiller renormalization factors of the SU(4) t - J model and the corresponding renormalized Hamiltonian. Utilizing the RVB state as a trial wave function and the mean-field approximation to this renormalized Hamiltonian on the honeycomb lattice case, we find that the extended s -wave state is much more favorable than the $d \pm id$ state in the doping region close to quarter filling, and the superconductivity almost disappears in the doping region close to half-filling. The spin-singlet pairing and the spin-triplet pairing can exist simultaneously in the pairing state of the SU(4) case.

ACKNOWLEDGMENTS

We thank Fu-Chun Zhang, Jian Kang, and Ting-Kuo Lee for helpful discussions. This work is supported by the National Key Research and Development Program of China (Grants Nos. 2017YFA0304204 and 2016YFA0300504), the National Natural Science Foundation of China Grant No. 11625416, and the Shanghai Municipal Government (Grants Nos. 19XD1400700 and 19JC1412702).

Appendix A: The Bogoliubov-de Gennes method

The expectation value of the renormalized Hamiltonian is

$$\begin{aligned} \langle \Psi_0 | H' | \Psi_0 \rangle = & -tg_t^{SU(4)} \sum_{\langle i,j \rangle} \sum_{\alpha=1}^4 (\chi_{\langle i,j \rangle \alpha} + \text{h.c.}) \\ & - \frac{5}{4} Jg_S^{SU(4)} \sum_{\langle i,j \rangle} \left(\langle \vec{\Delta}_{ij} \rangle_0 \right)^\dagger \cdot \langle \vec{\Delta}_{ij} \rangle_0 \\ & - \frac{15}{4} Jg_S^{SU(4)} \sum_{\langle i,j \rangle} \left(\sum_{\alpha} \chi_{\langle i,j \rangle \alpha}^* \sum_{\beta} \chi_{\langle i,j \rangle \beta} \right). \end{aligned} \quad (\text{A1})$$

We minimize the energy under the constraints $\sum_i \langle \Psi_0 | \hat{n}_i | \Psi_0 \rangle = N_e$, $\langle \Psi_0 | \Psi_0 \rangle = 1$, where N_e is the total number of electrons. Namely, minimizing the function $W = \langle \Psi_0 | H' | \Psi_0 \rangle - \lambda (\langle \Psi_0 | \Psi_0 \rangle - 1) - \mu (\sum_i \langle \Psi_0 | \hat{n}_i | \Psi_0 \rangle - N_e)$

which yields the variational relation

$$\begin{aligned}
0 &= \frac{\delta W}{\delta \langle \Psi_0 |} \\
&= \sum_{\langle i,j \rangle, \alpha} \frac{\partial W}{\partial \chi_{\langle i,j \rangle, \alpha}} \frac{\delta \chi_{\langle i,j \rangle, \alpha}}{\delta \langle \Psi_0 |} + \text{h.c.} \\
&\quad + \sum_{\langle i,j \rangle, \alpha\beta} \frac{\partial W}{\partial \Delta_{\langle i,j \rangle, \alpha\beta}} \frac{\delta \Delta_{\langle i,j \rangle, \alpha\beta}}{\delta \langle \Psi_0 |} + \text{h.c.} \\
&\quad + \sum_i \frac{\partial W}{\partial n_i} \frac{\delta n_i}{\delta \langle \Psi_0 |} - \lambda |\Psi_0\rangle, \tag{A2}
\end{aligned}$$

where $n_i = \langle \Psi_0 | \hat{n}_i | \Psi_0 \rangle$. For an operator \hat{O} , $\delta \langle \Psi_0 | \hat{O} | \Psi_0 \rangle / \delta \langle \Psi_0 | = \hat{O} | \Psi_0 \rangle$. Therefore we obtain the Schrödinger equation $H_{\text{MF}} | \Psi_0 \rangle = \lambda | \Psi_0 \rangle$ and

$$\begin{aligned}
H_{\text{MF}} &= \sum_{\langle i,j \rangle, \alpha} \frac{\partial W}{\partial \chi_{\langle i,j \rangle, \alpha}} c_{i,\alpha}^\dagger c_{j,\alpha} + \text{h.c.} \\
&\quad + \sum_{\langle i,j \rangle, \alpha\beta}^{\alpha \neq \beta} \frac{\partial W}{\partial \Delta_{\langle i,j \rangle, \alpha\beta}} c_{i,\alpha} c_{j,\beta} + \text{h.c.} + \sum_{i,\alpha} \frac{\partial W}{\partial n_i} \hat{n}_{i,\alpha}. \tag{A3}
\end{aligned}$$

Here

$$\frac{\partial W}{\partial n_i} = \frac{\partial W}{\partial n} = -\mu + \left[\frac{\partial \langle \Psi_0 | H' | \Psi_0 \rangle}{\partial n} \right]_g, \tag{A4}$$

$$\frac{\partial W}{\partial \chi_{\langle i,j \rangle, \alpha}} = -t g_t^{SU(4)} - \frac{15}{4} J g_S^{SU(4)} \sum_{\alpha} \chi_{\langle i,j \rangle, \alpha}^*, \tag{A5}$$

$$\frac{\partial W}{\partial \Delta_{\langle i,j \rangle, \alpha\beta}} = \frac{5}{2} J g_S^{SU(4)} (\Delta_{\langle i,j \rangle, \beta\alpha}^* - \Delta_{\langle i,j \rangle, \alpha\beta}^*), \tag{A6}$$

where $\left[\frac{\partial \langle \Psi_0 | H' | \Psi_0 \rangle}{\partial n} \right]_g$ in Eq. (A4) being the derivate of $\langle \Psi_0 | H' | \Psi_0 \rangle$ with respect to n via the renormalization g -factors and $\alpha \neq \beta$ in Eq. (A6). $-\partial W / \partial n$ can be viewed as the effective chemical potential and we let $\tilde{\mu} = -\partial W / \partial n$. For simplicity, in this paper we only consider real $\chi_{\langle i,j \rangle, \alpha}$. On the honeycomb lattice, for convenience, Eq. (A3) can be rewritten as

$$\begin{aligned}
H_{\text{MF}} &= \sum_{\langle i,j \rangle, \alpha} \frac{\partial W}{\partial \chi_{\langle i,j \rangle, \alpha}} c_{i,\alpha}^\dagger d_{j,\alpha} + \text{h.c.} \\
&\quad + \sum_{\langle i,j \rangle, \alpha\beta}^{\alpha \neq \beta} \frac{\partial W}{\partial \Delta_{\langle i,j \rangle, \alpha\beta}} c_{i,\alpha} d_{j,\beta} + \text{h.c.} - \tilde{\mu} \sum_{i,\alpha} \hat{n}_{i,\alpha}. \tag{A7}
\end{aligned}$$

Here we denote by d and c the electron annihilation operators related with the A and B sublattices of the honeycomb lattice, respectively. We can Fourier-transform the

Hamiltonian and diagonalize the kinetic part by using the trick [30] as follows:

$$\begin{aligned}
c_{\mathbf{k}\alpha} &= \frac{1}{\sqrt{2}} (f_{\mathbf{k}\alpha} + g_{\mathbf{k}\alpha}), \\
d_{\mathbf{k}\alpha} &= \frac{1}{\sqrt{2}} e^{-i\phi_{\mathbf{k}}} (f_{\mathbf{k}\alpha} - g_{\mathbf{k}\alpha}), \tag{A8}
\end{aligned}$$

where $\phi_{\mathbf{k}} = \arg(\gamma_{\mathbf{k}})$ and $\gamma_{\mathbf{k}} = \sum_{m=1}^3 e^{-i\mathbf{k} \cdot \vec{\tau}_m}$. Here $\vec{\tau}_m$, with $m = 1, 2, 3$, denotes the three nearest neighbour bond directions of the A site. Finally we obtain

$$H_{\text{MF}} = \sum_{\mathbf{k}} H_{\mathbf{k}} - \sum_{\mathbf{k}} \sum_{\alpha} 2\tilde{\mu}, \tag{A9}$$

with

$$\begin{aligned}
H_{\mathbf{k}} &= \sum_{\alpha} \frac{1}{2} [(\epsilon_{\mathbf{k}} - \tilde{\mu}) f_{\mathbf{k}\alpha}^\dagger f_{\mathbf{k}\alpha} + (-\epsilon_{\mathbf{k}} - \tilde{\mu}) g_{\mathbf{k}\alpha}^\dagger g_{\mathbf{k}\alpha}] \\
&\quad - \sum_{\alpha} \frac{1}{2} [(\epsilon_{\mathbf{k}} - \tilde{\mu}) f_{-\mathbf{k}\alpha}^\dagger f_{-\mathbf{k}\alpha} + (-\epsilon_{\mathbf{k}} - \tilde{\mu}) g_{-\mathbf{k}\alpha}^\dagger g_{-\mathbf{k}\alpha}] \\
&\quad - \frac{5}{4} J g_S^{SU(4)} \sum_{\alpha\beta}^{\alpha \neq \beta} [\Delta_{\mathbf{k}, \alpha\beta}^i (f_{\mathbf{k}\alpha}^\dagger f_{-\mathbf{k}\beta}^\dagger - g_{\mathbf{k}, \alpha}^\dagger g_{-\mathbf{k}\beta}^\dagger) + \text{h.c.}] \\
&\quad - \frac{5}{4} J g_S^{SU(4)} \sum_{\alpha\beta}^{\alpha \neq \beta} [\Delta_{\mathbf{k}, \alpha\beta}^I (f_{\mathbf{k}\alpha}^\dagger g_{-\mathbf{k}\beta}^\dagger - g_{\mathbf{k}, \alpha}^\dagger f_{-\mathbf{k}\beta}^\dagger) + \text{h.c.}], \tag{A10}
\end{aligned}$$

where $\epsilon_{\mathbf{k}} = |\gamma_{\mathbf{k}}| \partial W / \partial \chi_{\langle i,j \rangle, \alpha}$ and

$$\begin{aligned}
\Delta_{\mathbf{k}, \alpha\beta}^i &= -\tilde{\Delta}_{\alpha\beta}^i \Gamma_{\mathbf{k}}^i, \\
\Delta_{\mathbf{k}, \alpha\beta}^I &= -\tilde{\Delta}_{\alpha\beta}^I \Gamma_{\mathbf{k}}^I, \\
\Gamma_{\mathbf{k}}^i &= \sum_{m=1}^3 e^{i\varphi(m-1)} \cos(\mathbf{k} \cdot \vec{\tau}_m + \phi_{\mathbf{k}}), \\
\Gamma_{\mathbf{k}}^I &= \sum_{m=1}^3 e^{i\varphi(m-1)} i \sin(\mathbf{k} \cdot \vec{\tau}_m + \phi_{\mathbf{k}}), \\
\tilde{\Delta}_{\alpha\beta} &= \tilde{\Delta}_{\alpha\beta}^{\vec{\tau}_1}, \\
\tilde{\Delta}_{\alpha\beta}^{\vec{\tau}} &= \langle \Psi_0 | c_{\mathbf{R}_i + \vec{\tau}, \alpha} d_{\mathbf{R}_i, \beta} - c_{\mathbf{R}_i + \vec{\tau}, \beta} d_{\mathbf{R}_i, \alpha} | \Psi_0 \rangle. \tag{A11}
\end{aligned}$$

Here φ represents the phase difference between the pairing order parameters in the three nearest neighbour bond directions, namely, $\tilde{\Delta}_{\alpha\beta}^{\vec{\tau}_2} = e^{i\varphi} \tilde{\Delta}_{\alpha\beta}^{\vec{\tau}_1}$ and $\tilde{\Delta}_{\alpha\beta}^{\vec{\tau}_3} = e^{i2\varphi} \tilde{\Delta}_{\alpha\beta}^{\vec{\tau}_1}$. According to crystal field theory, in the two-dimensional hexagonal lattice there are only the $d \pm id$ state and extended s -wave state which are reasonable and favorable [28, 29]. $\varphi = 2\pi/3$ yields the $d \pm id$ state and $\varphi = 0$ yields the extended s -wave state. By using the sixteen-component notation $\tilde{f}_{\mathbf{k}} = (f_{\mathbf{k}\alpha}, \tilde{g}_{\mathbf{k}\alpha}, \tilde{f}_{-\mathbf{k}\alpha}^\dagger, \tilde{g}_{-\mathbf{k}\alpha}^\dagger)^T$ (for convenience here $\tilde{f}_{\mathbf{k}\alpha} = (f_{\mathbf{k}1}, f_{\mathbf{k}2}, f_{\mathbf{k}3}, f_{\mathbf{k}4})$ and $\tilde{g}_{-\mathbf{k}\alpha}^\dagger = (g_{-\mathbf{k}1}^\dagger, g_{-\mathbf{k}2}^\dagger, g_{-\mathbf{k}3}^\dagger, g_{-\mathbf{k}4}^\dagger)$) we can rewrite $H_{\mathbf{k}}$ as

$$H_{\mathbf{k}} = \tilde{f}_{\mathbf{k}}^\dagger \hat{\mathcal{E}}_{\mathbf{k}} \tilde{f}_{\mathbf{k}}, \tag{A12}$$

and

$$\hat{\mathcal{E}}_{\mathbf{k}} = \begin{bmatrix} \hat{\epsilon}_{\mathbf{k}}/2 & \hat{\Delta}_{\mathbf{k}} \\ \hat{\Delta}_{\mathbf{k}}^\dagger & -\hat{\epsilon}_{\mathbf{k}}/2 \end{bmatrix}, \quad (\text{A13})$$

where

$$\begin{aligned} \hat{\epsilon}_{\mathbf{k}} &= \begin{bmatrix} (\epsilon_{\mathbf{k}} - \tilde{\mu})\mathbf{1}_{4 \times 4} & 0 \\ 0 & (-\epsilon_{\mathbf{k}} - \tilde{\mu})\mathbf{1}_{4 \times 4} \end{bmatrix}, \\ \hat{\Delta}_{\mathbf{k}} &= \begin{bmatrix} \hat{L}_{\mathbf{k}} & \hat{R}_{\mathbf{k}} \\ -\hat{R}_{\mathbf{k}} & -\hat{L}_{\mathbf{k}} \end{bmatrix}, \\ (\hat{L}_{\mathbf{k}})_{\alpha\beta} &= \begin{cases} -\frac{5}{4}Jg_S^{SU(4)}\Delta_{\mathbf{k},\alpha\beta}^i & (\alpha \neq \beta) \\ 0 & (\alpha = \beta) \end{cases}, \\ (\hat{R}_{\mathbf{k}})_{\alpha\beta} &= \begin{cases} -\frac{5}{4}Jg_S^{SU(4)}\Delta_{\mathbf{k},\alpha\beta}^I & (\alpha \neq \beta) \\ 0 & (\alpha = \beta) \end{cases}. \end{aligned} \quad (\text{A14})$$

Note that we have the relation $\hat{\Delta}_{\mathbf{k}} = -\hat{\Delta}_{-\mathbf{k}}^T$. We can diagonalize $H_{\mathbf{k}}$ as follows:

$$H_{\mathbf{k}} = \sum_{n=1}^8 (E_{\mathbf{k}n} a_{\mathbf{k}n}^\dagger a_{\mathbf{k}n} - E_{-\mathbf{k}n} a_{-\mathbf{k}n} a_{-\mathbf{k}n}^\dagger), \quad (\text{A15})$$

by the (unitary) Bogoliubov transformation [28],

$$\begin{aligned} f_{\mathbf{k}\alpha} &= \sum_n^l \left(u_{f\alpha,n}^{\mathbf{k}} a_{\mathbf{k}n} + (v_{f\alpha,n}^{-\mathbf{k}})^* a_{-\mathbf{k}n}^\dagger \right), \\ g_{\mathbf{k}\alpha} &= \sum_n^l \left(u_{g\alpha,n}^{\mathbf{k}} a_{\mathbf{k}n} + (v_{g\alpha,n}^{-\mathbf{k}})^* a_{-\mathbf{k}n}^\dagger \right), \end{aligned} \quad (\text{A16})$$

where $a_{\mathbf{k}n}$ and $a_{\mathbf{k}n}^\dagger$ ($n=1,2,3,\dots,8$) satisfy the anticommutation relations of fermions ($\{a_{\mathbf{k}n}, a_{\mathbf{k}'m}^\dagger\} = \delta_{\mathbf{k}\mathbf{k}'}\delta_{nm}$, $\{a_{\mathbf{k}n}, a_{\mathbf{k}'m}\} = 0$) and generate the elementary excitations of the system. The prime sign above summation implies only those states with positive energy are counted. With the help of the sixteen-component notation $\mathbf{a}_{\mathbf{k}} = (a_{\mathbf{k}1}, \dots, a_{\mathbf{k}8}, a_{-\mathbf{k}1}^\dagger, \dots, a_{-\mathbf{k}8}^\dagger)^T$ we can obtain a more compact formulation of Eq. (A16): $\tilde{f}_{\mathbf{k}} = U_{\mathbf{k}} \mathbf{a}_{\mathbf{k}}$ with

$$U_{\mathbf{k}} = \begin{bmatrix} \hat{u}^{\mathbf{k}} & (\hat{v}^{-\mathbf{k}})^* \\ \hat{v}^{\mathbf{k}} & (\hat{u}^{-\mathbf{k}})^* \end{bmatrix} \quad \text{and} \quad U_{\mathbf{k}} U_{\mathbf{k}}^\dagger = \mathbf{1}. \quad (\text{A17})$$

Here 8×8 Bogoliubov transformation matrices $\hat{u}^{\mathbf{k}}$ and $\hat{v}^{\mathbf{k}}$ are defined by Eq. (A16). Using this formalism, we rewrite the Eq. (A15) as

$$U_{\mathbf{k}}^\dagger \hat{\mathcal{E}}_{\mathbf{k}} U_{\mathbf{k}} = \hat{E}_{\mathbf{k}}, \quad (\text{A18})$$

where $\hat{E}_{\mathbf{k}} = \text{diag}(E_{\mathbf{k}1}, \dots, E_{\mathbf{k}8}, -E_{-\mathbf{k}1}, \dots, -E_{-\mathbf{k}8})$. Therefore we obtain the Bogoliubov-de Gennes (BdG) [33] equations as follows:

$$\hat{\mathcal{E}}_{\mathbf{k}} \begin{pmatrix} \frac{u_{\cdot n}^{\mathbf{k}}}{v_{\cdot n}^{\mathbf{k}}} \end{pmatrix} = E_{\mathbf{k}n} \begin{pmatrix} \frac{u_{\cdot n}^{\mathbf{k}}}{v_{\cdot n}^{\mathbf{k}}} \end{pmatrix}. \quad (\text{A19})$$

Here $u_{\cdot n}^{\mathbf{k}}(v_{\cdot n}^{\mathbf{k}})$ is the n -th column of $\hat{u}^{\mathbf{k}}(\hat{v}^{\mathbf{k}})$. From Eq. (A19) we can know that if $\frac{u_{\cdot n}^{\mathbf{k}}}{v_{\cdot n}^{\mathbf{k}}}, E_{\mathbf{k}n}$ is the solution then $\frac{(v_{\cdot n}^{-\mathbf{k}})^*}{(u_{\cdot n}^{-\mathbf{k}})^*}, -E_{-\mathbf{k}n}$ is also the solution. This property is consistent with the unitary Bogoliubov transformation Eq. (A16). Note that $\langle \Psi_0 | a_{\mathbf{k}n}^\dagger a_{\mathbf{k}'m} | \Psi_0 \rangle = \delta_{\mathbf{k}\mathbf{k}'} \delta_{nm} f(2E_{\mathbf{k}n})$, $\langle \Psi_0 | a_{\mathbf{k}n} a_{\mathbf{k}m} | \Psi_0 \rangle = 0$ and $f(2E_{\mathbf{k}n}) = (\exp(2E_{\mathbf{k}n}/k_B T) + 1)^{-1}$. Our treatment is limited to zero temperature and thus we obtain the self consistent equations for the order parameters

$$\begin{aligned} \tilde{\Delta}_{\alpha\beta} &= (2N_s)^{-1} \sum_{\mathbf{k}} e^{i(\phi_{\mathbf{k}} + \mathbf{k} \cdot \bar{\tau}_1)} \sum_n^l [u_{f\alpha,n}^{\mathbf{k}} (v_{f\beta,n}^{\mathbf{k}})^* - u_{f\beta,n}^{\mathbf{k}} (v_{f\alpha,n}^{\mathbf{k}})^* - u_{g\alpha,n}^{\mathbf{k}} (v_{g\beta,n}^{\mathbf{k}})^* + u_{g\beta,n}^{\mathbf{k}} (v_{g\alpha,n}^{\mathbf{k}})^* \\ &\quad - u_{f\alpha,n}^{\mathbf{k}} (v_{g\beta,n}^{\mathbf{k}})^* + u_{g\alpha,n}^{\mathbf{k}} (v_{f\beta,n}^{\mathbf{k}})^* + u_{f\beta,n}^{\mathbf{k}} (v_{g\alpha,n}^{\mathbf{k}})^* - u_{g\beta,n}^{\mathbf{k}} (v_{f\alpha,n}^{\mathbf{k}})^*], \quad (\alpha \neq \beta) \\ \chi &= (2N_s)^{-1} \sum_{\alpha} \sum_{\mathbf{k}} \frac{1}{2} e^{-i(\phi_{\mathbf{k}} + \mathbf{k} \cdot \bar{\tau}_1)} \sum_n^l [|v_{f\alpha,n}^{-\mathbf{k}}|^2 - |v_{g\alpha,n}^{-\mathbf{k}}|^2 + (v_{f\alpha,n}^{-\mathbf{k}})^* v_{g\alpha,n}^{-\mathbf{k}} - v_{f\alpha,n}^{-\mathbf{k}} (v_{g\alpha,n}^{-\mathbf{k}})^* + \text{h.c.}], \\ n &= (2N_s)^{-1} \sum_{\alpha} \sum_{\mathbf{k}} \sum_n^l (|v_{f\alpha,n}^{-\mathbf{k}}|^2 + |v_{g\alpha,n}^{-\mathbf{k}}|^2), \end{aligned} \quad (\text{A20})$$

where $2N_s$ is the total number of sites. $\chi = \sum_{\alpha} (\chi_{\langle i,j \rangle \alpha} + \chi_{\langle i,j \rangle \alpha}^*)/2$ and $n = \sum_{\alpha} \langle \Psi_0 | d_{\mathbf{R}_i, \alpha}^\dagger d_{\mathbf{R}_i, \alpha} + c_{\mathbf{R}_i + \bar{\tau}_1, \alpha}^\dagger c_{\mathbf{R}_i + \bar{\tau}_1, \alpha} | \Psi_0 \rangle / 2$.

Appendix B: Pairing field flavor configurations of states

About the pairing field we have the relation

$$\begin{aligned} \vec{\Delta}_{ij} &= \tilde{c}_i^t (-\sigma^{32}, i\sigma^{02}, \sigma^{12}, -\sigma^{23}, i\sigma^{20}, \sigma^{21}) \tilde{c}_j \\ &= \tilde{c}_i^t (i\hat{\sigma}\sigma^2 \otimes \sigma^2, \sigma^2 \otimes i\hat{\sigma}\sigma^2) \tilde{c}_j, \end{aligned} \quad (\text{B1})$$

where $\hat{\sigma} = \sigma^1 \hat{e}_1 + \sigma^2 \hat{e}_2 + \sigma^3 \hat{e}_3$. With respect to pairing order parameters, its expectation value within the unprojected state Ψ_0 can be written as

$$\langle \vec{\Delta}_{\mathbf{R}_i + \vec{\tau}_1, \mathbf{R}_i} \rangle_0 = \left(i(\tilde{\Delta}_{12} - \tilde{\Delta}_{34}), (\tilde{\Delta}_{12} + \tilde{\Delta}_{34}), -i(\tilde{\Delta}_{14} - \tilde{\Delta}_{23}), i(\tilde{\Delta}_{13} - \tilde{\Delta}_{24}), (\tilde{\Delta}_{13} + \tilde{\Delta}_{24}), -i(\tilde{\Delta}_{14} + \tilde{\Delta}_{23}) \right). \quad (\text{B2})$$

Here \mathbf{R}_i represents the site of A sublattice of the honeycomb lattice. We insert the flavor configuration $\tilde{\Delta} = \tilde{\Delta}_{12} = \tilde{\Delta}_{34} = \tilde{\Delta}_{14} = \tilde{\Delta}_{23} = \tilde{\Delta}_{13} = -\tilde{\Delta}_{24}$ introduced in our paper into Eq. (B2) to obtain

$$\begin{aligned} \langle \vec{\Delta}_{\mathbf{R}_i + \vec{\tau}_1, \mathbf{R}_i} \rangle_0 &= \left(0, 2\tilde{\Delta}, 0, 2i\tilde{\Delta}, 0, -2i\tilde{\Delta} \right) \\ &= \langle \tilde{c}_i^t (0, i\sigma^{02}, 0, -\sigma^{23}, 0, \sigma^{21}) \tilde{c}_j \rangle_0. \end{aligned} \quad (\text{B3})$$

Using v_1 and v_2 as the orbital index, we choose the representation $\tilde{c}_j = (c_{j\uparrow v_1}, c_{j\uparrow v_2}, c_{j\downarrow v_1}, c_{j\downarrow v_2})^t$. According to Eq. (B1), the previous three components of Eq. (B3) describe spin triplet with $d_y \neq 0, d_x = d_z = 0$ and orbital singlet, where \mathbf{d} is the vector defined by triplet pairing

$$\begin{aligned} \hat{\Delta}(\mathbf{k}) &= i(\mathbf{d}(\mathbf{k}) \cdot \hat{\sigma})\sigma^2 \\ &= \begin{pmatrix} -d_x(\mathbf{k}) + id_y(\mathbf{k}) & d_z(\mathbf{k}) \\ d_z(\mathbf{k}) & d_x(\mathbf{k}) + id_y(\mathbf{k}) \end{pmatrix}. \end{aligned} \quad (\text{B4})$$

$$\langle \vec{\Delta}_{\mathbf{R}_i + \vec{\tau}_1, \mathbf{R}_i} \rangle_0 = \left(i\tilde{\Delta}_{12}(1 - e^{i\theta_1}), \tilde{\Delta}_{12}(1 + e^{i\theta_1}), -i\tilde{\Delta}_{14}(1 - e^{i\theta_3}), i\tilde{\Delta}_{13}(1 + e^{i\theta_2}), \tilde{\Delta}_{13}(1 - e^{\theta_2}), -i\tilde{\Delta}_{14}(1 + e^{i\theta_3}) \right). \quad (\text{B6})$$

We can clearly see that when $\theta_i \neq 0, \pi, (i = 1, 2, 3)$,

The last three components of Eq. (B3) describe spin singlet and orbital triplet with $d_y = 0, d_x \neq 0, d_z \neq 0$. Note that the spin singlet pairing and the spin triplet pairing coexist simultaneously in this flavor configuration. If we insert another flavor configuration $\tilde{\Delta} = \tilde{\Delta}_{12} = -\tilde{\Delta}_{34} = \tilde{\Delta}_{14} = -\tilde{\Delta}_{23} = \tilde{\Delta}_{13} = \tilde{\Delta}_{24}$ into Eq. (B2), we will obtain

$$\begin{aligned} \langle \vec{\Delta}_{\mathbf{R}_i + \vec{\tau}_1, \mathbf{R}_i} \rangle_0 &= \left(2i\tilde{\Delta}, 0, -2i\tilde{\Delta}, 0, 2\tilde{\Delta}, 0 \right) \\ &= \langle \tilde{c}_i^t (-\sigma^{32}, 0, \sigma^{12}, 0, i\sigma^{20}, 0) \tilde{c}_j \rangle_0. \end{aligned} \quad (\text{B5})$$

This indicates that there is symmetry between the spin index and the orbital index. As mentioned in our paper, there is the gauge redundancy. Namely, $c_1 \rightarrow c'_1 = c_1 e^{i(\theta_1 + \theta_2 + 2\theta_4)/2}$, $c_2 \rightarrow c'_2 = c_2 e^{i(\theta_1 - \theta_3 + 2\theta_4)/2}$, $c_3 \rightarrow c'_3 = c_3 e^{i(\theta_2 - \theta_3 + 2\theta_4)/2}$, and $c_4 \rightarrow c'_4 = c_4 e^{i\theta_4}$, then we obtain $\tilde{\Delta}_{12} = e^{-i\theta_1} \tilde{\Delta}_{34}$, $\tilde{\Delta}_{14} = e^{-i\theta_3} \tilde{\Delta}_{23}$, and $\tilde{\Delta}_{13} = -e^{-i\theta_2} \tilde{\Delta}_{24}$. And insert this general flavor configuration into Eq. (B2) to obtain

the six components of $\langle \vec{\Delta}_{\mathbf{R}_i + \vec{\tau}_1, \mathbf{R}_i} \rangle_0$ are simultaneously nonvanishing.

-
- [1] P. W. Anderson, *Science* **235**, 1196 (1987).
[2] Y. Q. Li, M. Ma, D. N. Shi, and F. C. Zhang, *Phys. Rev. Lett.* **81**, 3527 (1998).
[3] Z. Zhou, D. Wang, Z. Y. Meng, Y. Wang, and C. Wu, *Phys. Rev. B* **93**, 245157 (2016).
[4] C. Xu and L. Balents, *Phys. Rev. Lett.* **121**, 087001 (2018).
[5] M. G. Yamada, M. Oshikawa, and G. Jackeli, *Phys. Rev. Lett.* **121**, 097201 (2018).
[6] Y. Cao, V. Fatemi, S. Fang, K. Watanabe, T. Taniguchi, E. Kaxiras, and P. Jarillo-Herrero, *Nature* **556**, 43 (2018).
[7] Y. Cao, V. Fatemi, A. Demir, S. Fang, S. L. Tomarken, J. Y. Luo, J. D. Sanchez-Yamagishi, K. Watanabe, T. Taniguchi, E. Kaxiras, et al., *Nature* **556**, 80 (2018).
[8] N. F. Q. Yuan and L. Fu, *Phys. Rev. B* **98**, 045103 (2018).
[9] M. Koshino, N. F. Q. Yuan, T. Koretsune, M. Ochi, K. Kuroki, and L. Fu, *Phys. Rev. X* **8**, 031087 (2018).
[10] Z. Zhu, D. N. Sheng, and L. Fu, *Phys. Rev. Lett.* **123**, 087602 (2019).
[11] H. C. Po, L. Zou, A. Vishwanath, and T. Senthil, *Phys. Rev. X* **8**, 031089 (2018).
[12] X. Y. Xu, K. T. Law, and P. A. Lee, *Phys. Rev. B* **98**, 121406 (2018).
[13] J. F. Dodaro, S. A. Kivelson, Y. Schattner, X. Q. Sun, and C. Wang, *Phys. Rev. B* **98**, 075154 (2018).
[14] C.-C. Liu, L.-D. Zhang, W.-Q. Chen, and F. Yang, *Phys. Rev. Lett.* **121**, 217001 (2018).
[15] J. Kang and O. Vafek, *Phys. Rev. X* **8**, 031088 (2018).

- [16] J. González and T. Stauber, *Phys. Rev. Lett.* **122**, 026801 (2019).
- [17] D. M. Kennes, J. Lischner, and C. Karrasch, *Phys. Rev. B* **98**, 241407 (2018).
- [18] Q.-K. Tang, L. Yang, D. Wang, F.-C. Zhang, and Q.-H. Wang, *Phys. Rev. B* **99**, 094521 (2019).
- [19] B. Roy and V. Juričić, *Phys. Rev. B* **99**, 121407 (2019).
- [20] V. Kozii, H. Isobe, J. W. F. Venderbos, and L. Fu, *Phys. Rev. B* **99**, 144507 (2019).
- [21] M. Yankowitz, S. Chen, H. Polshyn, Y. Zhang, K. Watanabe, T. Taniguchi, D. Graf, A. F. Young, and C. R. Dean, *Science* **363**, 1059 (2019).
- [22] P. A. Lee, N. Nagaosa, and X.-G. Wen, *Rev. Mod. Phys.* **78**, 17 (2006).
- [23] F. C. Zhang, C. Gros, T. M. Rice, and H. Shiba, *Superconductor Science and Technology* **1**, 36 (1988).
- [24] I. F. Herbut, V. Juričić, and B. Roy, *Phys. Rev. B* **79**, 085116 (2009).
- [25] L. Savary, J. Ruhman, J. W. F. Venderbos, L. Fu, and P. A. Lee, *Phys. Rev. B* **96**, 214514 (2017).
- [26] B. Edegger, V. N. Muthukumar, and C. Gros, *Advances in Physics* **56**, 927 (2007).
- [27] K.-Y. Yang, W. Q. Chen, T. M. Rice, M. Sigrist, and F.-C. Zhang, *New Journal of Physics* **11**, 055053 (2009).
- [28] M. Sigrist and K. Ueda, *Rev. Mod. Phys.* **63**, 239 (1991).
- [29] A. M. Black-Schaffer and C. Honerkamp, *Journal of Physics: Condensed Matter* **26**, 423201 (2014).
- [30] W. Wu, M. M. Scherer, C. Honerkamp, and K. Le Hur, *Phys. Rev. B* **87**, 094521 (2013).
- [31] P. W. Anderson, P. A. Lee, M. Randeria, T. M. Rice, N. Trivedi, and F. C. Zhang, *Journal of Physics: Condensed Matter* **16**, R755 (2004).
- [32] M. Ogata and H. Fukuyama, *Rep. Prog. Phys.* **71**, 036501 (2008).
- [33] P. G. D. Gennes, *Superconductivity of Metals and Alloys*, Advanced book classics (Advanced Book Program, Perseus Books, 1999).